scientific reports

Check for updates

OPEN

Brain network hypersensitivity underlies pain crises in sickle cell disease

Pangyu Joo[1], Minkyung Kim[1], Brianna Kish[2], Vidhya Vijayakrishnan Nair[2], Yunjie Tong[2], Ziyue Liu[3,4], Andrew R. W. O'Brien[5], Steven E. Harte[6], Richard E. Harris[6,7], UnCheol Lee[1]✉ & Ying Wang[5,8]✉

Sickle cell disease (SCD) is a genetic disorder causing painful and unpredictable Vaso-occlusive crises (VOCs) through blood vessel blockages. In this study, we propose explosive synchronization (ES) as a novel approach to comprehend the hypersensitivity and occurrence of VOCs in the SCD brain network. We hypothesized that the accumulated disruptions in the brain network induced by SCD might lead to strengthened ES and hypersensitivity. We explored ES's relationship with patient reported outcome measures (PROMs) as well as VOCs by analyzing EEG data from 25 SCD patients and 18 matched controls. SCD patients exhibited lower alpha frequency than controls. SCD patients showed correlation between frequency disassortativity (FDA), an ES condition, and three important PROMs. Furthermore, stronger FDA was observed in SCD patients with a higher frequency of VOCs and EEG recording near VOC. We also conducted computational modeling on SCD brain network to study FDA's role in network sensitivity. Our model demonstrated that a stronger FDA could be linked to increased sensitivity and frequency of VOCs. This study establishes connections between SCD pain and the universal network mechanism, ES, offering a strong theoretical foundation. This understanding will aid predicting VOCs and refining pain management for SCD patients.

Sickle cell disease (SCD) is a common inherited blood disorder affecting 1 in 500 Black Americans. Pain in SCD is a lifelong major complication starting from infancy, and can be acute, chronic, or a mixture of both. Vaso-occlusive crises (VOCs) associated with SCD are extremely painful episodes that are recurrent, unpredictable, and frequently require hospitalization and opioids for pain control. Individuals with SCD that require high doses of opioids for VOCs have an increased risk of overdose and death, development of opioid-induced hyperalgesia, and lowered quality of life (QoL)[1]. The frequency of VOCs varies widely across SCD individuals with a recent systematic review reporting a range of 0–18 per year[2]. Recent studies suggest that the occurrence of VOCs is associated with abnormal vasoconstriction patterns resulting from dysfunction of the autonomic nervous system, endothelial dysfunction, and/or psychological stress[3–5]. Central nervous system (CNS) factors may also contribute to VOCs. For example, we showed that brain connectivity between the Default Mode Network (DMN) and structures of the Salience network were altered in SCD patients that had more VOCs[6]. Interestingly, this pattern of connectivity was consistent with that observed in fibromyalgia, a chronic widespread pain disorder accompanied by fatigue, sleep disturbance, and sensory hypersensitivity[7,8].

Explosive synchronization (ES) is a universal physical phenomenon wherein a small perturbation to a network can result in an abrupt state transition. The typical properties of an ES network include its high sensitivity to external stimuli and abrupt state transition at a tipping point[9,10]. Recent studies have suggested a link between

[1]Department of Anesthesiology, Center for Consciousness Science, Center for the Study of Complex Systems, Michigan Psychedelic Center, University of Michigan, Arbor Lakes Building 1 Suite 2200, 4251 Plymouth Road, Ann Arbor, MI 48105, USA. [2]Weldon School of Biomedical Engineering, Purdue University, West Lafayette, IN, USA. [3]Indiana Center for Musculoskeletal Health, Indiana University, Indianapolis, IN, USA. [4]Department of Biostatistics, Indiana University School of Medicine, Indianapolis, IN, USA. [5]Division of Hematology/Oncology, Department of Medicine, Indiana University School of Medicine, Indianapolis, IN, USA. [6]Department of Anesthesiology, Chronic Pain and Fatigue Research Center, University of Michigan, Ann Arbor, MI, USA. [7]Susan Samueli Integrative Health Institute, and Department of Anesthesiology and Perioperative Care, School of Medicine, University of California at Irvine, Irvine, CA, USA. [8]Department of Anesthesia, Stark Neurosciences Research Institute, Indiana University School of Medicine, Stark Neuroscience Building, Rm# 514E, 320 West 15th Street, Indianapolis, IN 46202, USA. ✉email: uclee@med.umich.edu; ywa12@iu.edu

ES in brain networks and chronic pain. We recently demonstrated that patients with fibromyalgia exhibit characteristics of ES on electroencephalography (EEG) that are associated with increased pain intensity[10], and that modulation of brain networks can transform a sensitive network into an insensitive one, or one not prone to ES[11]. These modeling investigations provided valuable insights into the network-level mechanisms of fibromyalgia and provide a rationale for studying ES mechanisms in other pain populations such as SCD.

In this study, we sought to extend our exploration of ES mechanisms into SCD. We hypothesized that changes in the brain network connectivity as observed in patients with SCD can potentially disrupt the hub structure, leading to ES and hypersensitivity. To test the hypothesis, we performed EEG on SCD patients and matched healthy controls. Furthermore, we examined differences in ES strength in SCD patients at various times before and after VOC events. Additionally, we developed a computational model to examine the relationship between ES and the occurrence of VOCs in the SCD brain.

Methods

Study design and participants

Thirty-two patients with SCD (16 male and 16 female) aged 14–73 years, and 18 pain-free ethnicity-, age- and gender-matched healthy controls (HCs) without SCD, were enrolled. All participants were Black or African American. Detailed inclusion and exclusion criteria can be found in Supplementary Table S1. In brief, the main inclusion criteria for SCD participants included: (1) experiencing chronic pain greater than or equal to 3/10 on most days for the past 6 months or at least one VOC in the past 12 months, (2) no recent history of initiating or adjusting the dose of stimulant medications in the past one month, and (3) willingness to maintain current SCD and pain treatments, and not to introduce any treatment for pain for the duration of study participation.

Each participant underwent an EEG recording following the administration of patient reported outcome measures (PROMs) and routine laboratory tests for complete blood cell count, reticulocytes, and hemoglobin electrophoresis. We were unable to collect quality EEG data from some SCD patients with thick curly hair that interfered with cap placement or those experiencing a pain flare on the day of recording, leading to increased noise during EEG measurements. EEG signal noise was primarily addressed during preprocessing; however, some recordings (n = 7) with severe noise could not be corrected and were excluded from analysis. Therefore, the final analysis sample was 25 (see Supplementary Fig. S1). The study was approved by the Institutional Review Board at Indiana University and conformed to the relevant ethical guidelines and regulations for human subjects' research. All adult patients and parents/guardians of pediatric patients provided written informed consent before participating in the study.

Concurrent EEG with pressure pain stimulator

EEG was performed in a quiet room using multi-channel BrainAmp MR (Brain Products GmBH, Gilching, Germany) and a noninvasive cutaneous electrode cap with conductive gel. After donning the cap, the participants were instructed to remain as still as possible for the entire procedure, to stay awake while their eyes were closed. Recordings were done with eyes closed during a state of rest or during concurrent pressure pain stimulation (individually calibrated to evoke moderate pain defined as a pain rating of ~ 40/100, i.e., Pain 40) that was elicited by a computerized pressure cuff (Hokanson, Bellevue, WA, USA) attached to the left gastrocnemius muscle. This method has been used previously to elicit evoked pressure pain in fibromyalgia patients[12]. First a resting state EEG was collected while participants rested with their eyes closed for 5 min. EEG was then recorded for 5-min during tonic pressure pain with eyes closed. Following the pressure pain protocol, resting state EEG recording was repeated for 5-min with eyes closed. Our previous EEG study[10] successfully demonstrated a significant correlation between ES strength and pain intensity in fibromyalgia patients using 5-min EEG data (300 s). Based on this prior success with similar analysis methods, we believed that 240-s EEG data may also be sufficient to investigate the relationship between ES strength and pain scores in SCD patients.

Patient reported outcome measures (PROMs)

Pain (pain intensity and interference) and physical function were assessed before EEG recordings with the Brief Pain Inventory (BPI)[13] and PROMIS-29[14]. The Fibromyalgia Survey Questionnaire (FSQ), which consists of the Widespread Pain Index and the Symptom Severity scale[15,16], was utilized as a surrogate measure of nociplastic pain. Anxiety and depression were evaluated using Hospital Anxiety and Depression Scale (HADS)[13]. The number of patient-reported VOCs in the preceding 12 months was documented, a method which is commonly used in pain research for SCD[6,17]. Pain-related QoL was evaluated using the Pediatric Quality of Life Inventory (PedsQL)[18].

EEG analysis

EEG preprocessing

In this study, we analyzed a 31 channel EEG (FP1, FP2, F3, F4, C3, C4, P3, P4, O1, O2, F7, F8, T7, T8, P7, P8, Fz, Cz, Pz, Oz, FC1, FC2, CP1, CP2, FC5, FC6, CP5, CP6, TP9, TP10 and POz), excluding an ECG channel (Fig. 1A). The raw EEG data were preprocessed using MATLAB and the EEGLAB toolbox[19]. First, a 0.5–59 Hz bandpass filter was applied to remove frequency bands with high levels of noise. Next, a visual inspection of the waveform and spectrogram of EEG was performed to remove channels with obvious noise and to segment the data into 240-s intervals. To minimize errors in spherical spline interpolation, data with more than 20% of channels removed were excluded in this study. Also, EEG data with a duration of less than 240 s was excluded from the analysis. With these criteria, data from 7 individuals were excluded out of the 32 SCD participants, leaving 25 participants' data for analysis. Among the HC group, no data was excluded with these criteria, leaving 18 participants' data for analysis. Next, Independent components with a significantly high probability (> 95%)

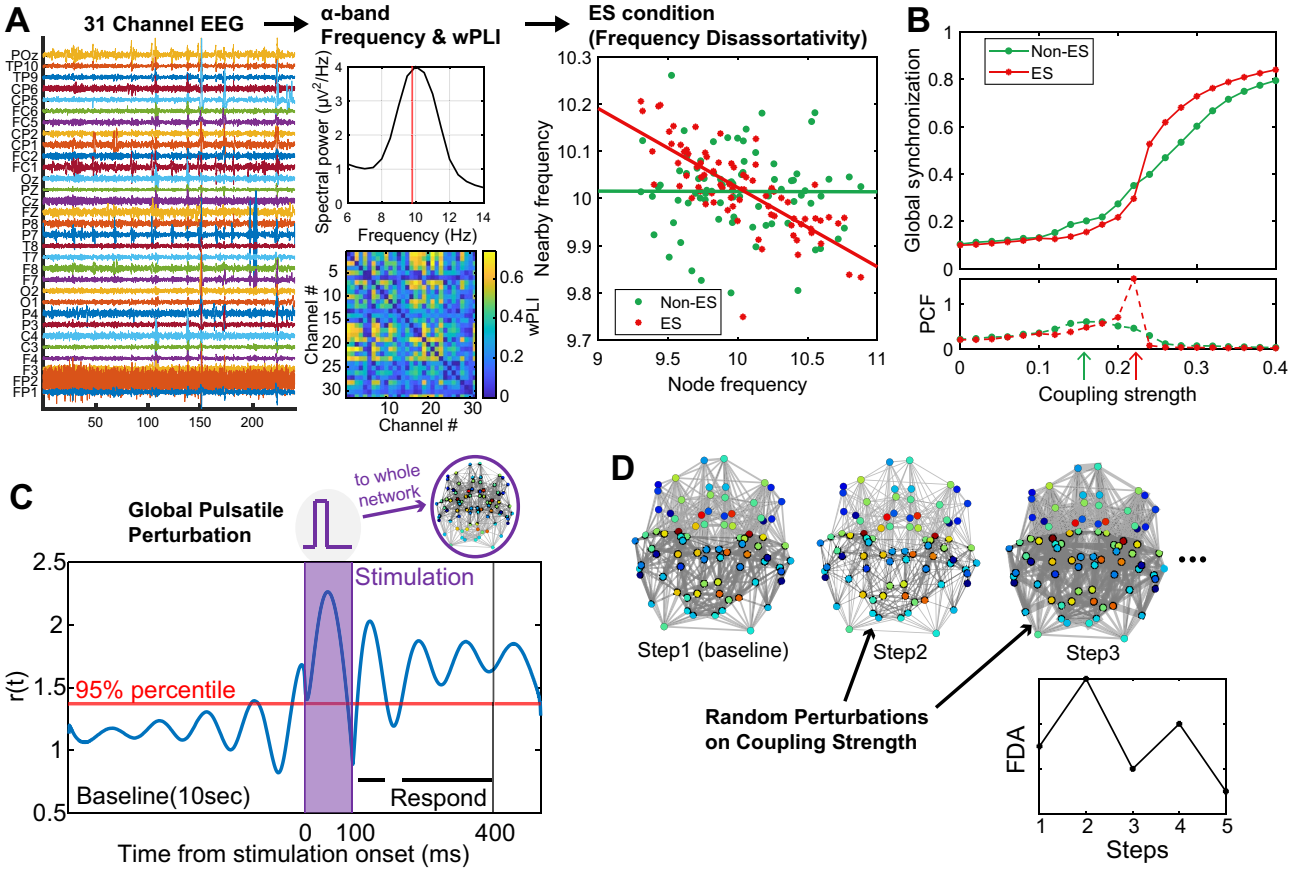

Figure 1. Schematic diagram of the study. (**A**) Schematic for the EEG analysis in this study. wPLI matrix and median frequency of alpha band were calculated from 31 channel EEG. FDA, one of the ES conditions, was obtained from wPLI network and median alpha frequency. (**B**) An example of synchronization characteristics of ES and non-ES network. The coupling strength at which the PCF reaches its maximum value was defined as critical point (green and red arrows). (**C**) An anatomical brain network and Stuart-Landau model were used to investigate the sensitivity and frequency of state transition of the brain network. Global Pulsatile perturbation is given for 100ms and the respond from the perturbation is measured from the subsequent 300ms. (**D**) Random perturbation on coupling strength is given to simulate number of state transitions under noisy environment. The difference in node colors in the brain network indicates the difference in node degrees.

being non-EEG were removed using runica in EEGLAB and IClabel[20]. The removed channels were recovered using spherical spline interpolation and finally the EEG was average referenced. In this study, we focused on analyzing alpha rhythms, which display distinct oscillatory patterns around 10 Hz and are known to be highly relevant to cognitive phenomena, including pain[21–24]. To achieve this, we utilized a band-pass filter and specifically analyzed the alpha band containing 7–13 Hz EEG signals.

Weighted phase lag index (wPLI)

Weighted phase lag index (wPLI) is used to assess functional connectivity from the phase difference between two-time series and is particularly robust to volume conditions commonly observed in EEG[25]. The wPLI between the *i*th and *j*th channels is defined by the following equation.

$$wPLI_{ij} = \frac{|\langle \sin\Delta\varphi_{ij} \rangle|}{\langle |\sin\Delta\varphi_{ij}| \rangle} = \frac{|\langle |\sin\Delta\varphi_{ij}| \mathrm{sign}(\sin\Delta\varphi_{ij}) \rangle|}{\langle |\sin\Delta\varphi_{ij}| \rangle},$$

Where $\Delta\varphi_{ij}$ represents phase difference between *i*th and *j*th channel band EEG. In this study, we utilized 240 s of alpha-band EEG (7–13 Hz) to evaluate individual patients' wPLI. We segmented the 240-s long EEG into 8 windows of 30 s. Then, we calculated the wPLI for each window and averaged the 8 wPLI values (240/30 = 8) to represent a patient's wPLI. The window size was determined to optimize differentiation between the HC and SCD groups (Supplementary Fig. S2).

Frequency disassortativity (FDA)

Frequency disassortativity (FDA) is one of the network conditions that can induce ES at a critical point. FDA refers to the tendency where high-frequency nodes are connected to low-frequency nodes, or vice versa, within a network[26,27]. FDA suppresses network synchronization, which competes with the opposite force to promote

synchronization at a critical point. If a network is at a critical point where the two competing forces are in balance (e.g., between healthy and pain states in the brain), the network is highly sensitive and exhibits abrupt state transition even with a small stimulus. Therefore, a network with a larger FDA makes the network more sensitive to external stimuli.

Defining a representative frequency for each EEG channel is necessary for the calculation of FDA. The most apparent method is to use the peak frequency, the frequency of the maximal power, in the alpha band (7–13 Hz). However, the peak frequency faces a limitation in cases where a clear peak is absent in alpha power spectrum, and particularly when estimating FDA, a feature of the entire network. Therefore, we used the median frequency of the alpha band to define the representative frequency of an EEG channel, and it enabled us to define representative frequencies for all the EEG channels. The 240-s EEG was segmented into eight 30-s windows, and in each window, the spectral power was computed using Welch's method (2-s window and 1-s overlapping). The median alpha frequency is defined as the 50% percentile of cumulative spectral power within the alpha band (7–13 Hz).

Furthermore, we constructed wPLI network in each 30-s window, which is required to determine the connections among EEG channels. The top 30% of the wPLI connections for all the pairs of EEG channels were deemed as significant functional connections. Then, the Spearman correlation coefficient (ρ_f) was calculated between the median alpha frequencies of the 31 EEG channels and the averaged median alpha frequencies of the neighboring EEG channels that are functionally connected to the 31 EEG channels. The negative Spearman correlation coefficient ρ_f indicates frequency disassortativity.

Computational modeling of SCD brain network

Stuart–Landau based brain model

We performed a computational model of the SCD brain in order to simulate altered ES function and test for sensitivity of network mechanisms. Stuart–Landau model is a mathematical model that describes the dynamics of coupled oscillator systems and their synchronization. The Stuart-Landau oscillator is extensively utilized for simulating the oscillatory dynamics between neural masses in the brain and for simulating brain signals from many different modalities[11,28,29]. In this study, we aim to investigate the sensitivity changes in the brain and the occurrence of crises using the Stuart–Landau model.

The coupled Stuart–Landau model is defined by the following equations.

$$\dot{r}_i(t) = \left\{\lambda_i - |r_i(t)|^2\right\} r_i(t) + S\sum_{j=1}^{N} A_{ij} r_j \cos\left[\theta_j\left(t-\tau_{ij}\right) - \theta_i(t)\right],$$

$$\dot{\theta}_i(t) = \omega_i + S\sum_{j=1}^{N} A_{ij}\frac{r_j}{r_i}\sin\left[\theta_j\left(t-\tau_{ij}\right) - \theta_i(t)\right],$$

where $r_i(t)$ and $\theta_i(t)$ are the amplitude and phase of ith oscillator, respectively.

λ_i is a parameter that determines the size of the limit cycle of the oscillator, and it was set to 1. ω_i determines the natural frequency of an ith oscillator and was normally distributed with 10 Hz mean and 0.4 Hz standard deviation to simulate alpha waves in the brain. A_{ij} represents the anatomical connectivity derived from diffusion tensor imaging (DTI), which has been parcellated into 82 nodes[30]. A_{ij} was binarized, limiting its values to either 0 or 1. The time delay $\tau_{ij} = D_{ij}/\upsilon$ represents the delay between region i and j, where D_{ij} denotes the distance between ith and jth brain regions. Here, υ is set to 7 ms, representing the average speed of axons across brain regions[31]. S represents the coupling strength between oscillators and S varied from 0 to 1.

To simulate the SCD brain activities in wakefulness, we assumed that the brain network resides near a critical state. A critical state is a balanced state between order and disorder, originally introduced in thermodynamics, but it has been widely studied in biological systems as an optimal state for information processing, especially highly informative, integrative, and flexible brain states of a conscious state[32–35]. To identify a critical point, we used the pair correlation function (PCF), which measures the variance of point-wise global phase synchronization (i.e., instantaneous order parameters)[36]. Since PCF is maximal at a critical point[36], we identified the maximal PCF as the critical point in this model study. When a network is closer to ES, the network undergoes a steeper transition near a critical point (Fig. 1B) and exhibits a high sensitivity to external perturbations. By varying the coupling strength S in increments of 0.005, we searched the maximal PCF and fixed S of the maximal PCF as the critical point of the brain network. Twenty iterations were conducted for each frequency distribution, changing the initial phase (r) and amplitude (θ), and the outcomes were tested statistically.

Modulation of model FDA

To create a brain network with a specific level of FDA, measured by the Spearman correlation (ρ_f) between individual node frequencies, $W=[\omega_1, \omega_2, \ldots, \omega_{82}]$, and their neighboring nodes' average frequencies, $nW=[n\omega_1, n\omega_2, \ldots, n\omega_{82}]$, we developed a new FDA algorithm. The neighboring nodes of the 82 nodes are determined by the anatomically informed brain network structure. The goal of this FDA algorithm is to configure the spatial arrangement of frequencies and make the brain network have a desired Spearman correlation between W and nW. The algorithm can be outlined as follows: (1) first assign frequencies randomly to each of the 82 nodes in the brain network, (2) calculate the Spearman correlation (ρ_f) between F and NF. If the ρ_f is below the target ρ_f, (3) randomly choose a node (i) from the 82 nodes, and determine the rank of its frequency ω_i within W (e.g., 3rd largest), (4) replace the frequency ω_i of that node (i) with the frequency ω_j of the node (j) whose $n\omega_j$ is the same rank in nW (the 3rd largest). (5) Go back to step 2 and repeat the process until the ρ_f between W and

nW reaches the desired ρ_f value. This usually takes about 200 iterations. The final brain network will exhibit the specific FDA level that was desired. Notably, previous algorithms altered model network structure to get a target FDA level[27,37]; however, in our model study, since the anatomical brain network structure was fixed, only by swapping the frequencies, we achieve the desired FDA level.

Sensitivity test

We conducted simulations for each frequency distribution with different FDA by placing the system at the critical state and applying pulsatile stimulation. By measuring the response to the pulsatile perturbation, we could simulate how the brain network sensitively responds to the external perturbations such as sensory input signals. To measure the sensitivity of the model brain network system, global pulsatile perturbations were applied, and the corresponding responses were measured (Fig. 1C)[38]. The pulsatile perturbation $u(t)$ was added to the amplitude equation, as shown in the following equation.

$$\dot{r}_i(t) = \left\{\lambda_i - |r_i(t)|^2\right\} r_i(t) + S\sum_{j=1}^{N} A_{ij} r_j \cos\left[\theta_j\left(t - \tau_{ij}\right) - \theta_i(t)\right] + u(t),$$

$$\dot{\theta}_i(t) = \omega_i + S\sum_{j=1}^{N} A_{ij}\frac{r_j}{r_i}\sin\left[\theta_j\left(t - \tau_{ij}\right) - \theta_i(t)\right].$$

An iteration lasted 25 s to exclude transient effects (10 s) and get a sufficient time for baseline estimate (10 s) with about 100 alpha wave cycles. The pulsatile perturbation was given at 20 s and lasted 100 ms to include a complete cycle of alpha oscillation. The amplitude of the pulsatile perturbation was 50 to give a perturbation that results in a measurable response without saturating the system. The simulations were done on 100 different initial frequency configurations and 20 iterations with different initial phases and amplitude. A perturbation response time series of ith node $PR_i(t)$ can be generated by applying a significance threshold of the 95th percentile to the amplitudes observed in the 10 s preceding the onset of stimulation. The values of $PR_i(t)$ are set to 1 for amplitudes exceeding the threshold and 0 otherwise. In other words, if the amplitude after stimulation exceeds the 95th percentile of the baseline, we consider it as a responded activity to the stimulus. Responsivity and complexity are defined as $\langle PR_i(t)\rangle$ and Lempel–Ziv complexity[39] of $PR_i(t)$ respectively. Responsivity measures the amount of the significant responses, and complexity measures how complex the patterns of the responses are. Responsivity and complexity are calculated using 300 ms of $PR_i(t)$ from the moment the pulsatile stimulation ends. The large responsivity and complexity after the stimulation means large sensitivity.

Simulation on the frequency of close crisis state

We performed modeling on the occurrence frequency of model VOCs to investigate the relationship between the ES strength and the frequency of VOC occurrence (Fig. 1D). Each simulation step lasted for 20 s, with normally distributed random constant perturbations (σ=5% of coupling strength at a critical point) given to the network coupling strength S in each period. That is, S in the Stuart-Landau equation is replaced by $S \times [1 + N(0, 0.05^2)]$. The FDA of each step was calculated using the median frequency of the last 10 s interval and DTI based anatomical network. This is referred to as the "signal FDA amplitude". Based on the results of EEG and VOC occurrence analysis, a state with signal FDA amplitude greater than 0.2 was defined as a "close crisis" state. We then counted the occurrences of the close crisis state among 100 steps. We conducted simulations of 20 brain networks with different initial frequency configurations in this scheme.

Statistical analyses

Statistical analysis was performed using either SPSS 29.0.1 or MATLAB. Demographic data were displayed as median and interquartile range. Two-sample t-tests were conducted on EEG characteristics between participants with SCD and matched healthy controls. Correlation analyses between frequency disassortativity and each of the PROMs were performed including age, sex and use of hydroxyurea as control covariables. Linear regression was constructed including frequency disassortativity as a dependent variable, "close to or distant from VOCs," and age, sex and use of hydroxyurea as predictors. P-values less than 0.05 were considered significant. The study is appropriately powered at greater than 0.84 with the current sample size of n = 25.

Results

Patient demographics

Thirty-two participants with SCD with eighteen age-, gender- and ethnicity-matched HCs underwent EEG recording following screening visit and enrolled on the study. PROMs were collected followed by EEG recordings within 1 week. Assessment of recording quality further excluded recordings from 7 participants (Supplementary Fig. S1). Study criteria for SCD was listed in Supplementary Table S1. Demographic information was displayed in Table 1. Participants with SCD and HCs did not differ in age, gender, height, and weight. Participants with SCD showed significantly higher levels of WBC, RBC, Hgb, Hct (%), Reticulocytes (%) and Hemoglobin A (%). Three participants were on chronic transfusion. Fifteen participants were receiving hydroxyurea. In line with the literature, participants with SCD showed elevated pain, pain interference, depression and physical dysfunction as compared to HCs (Table 1).

Subject characteristics	SCD (n = 25)	Healthy (n = 18)	P-value
Age (years), median (range)	37.00 (27.00–45.00)	38.00 (25.75–57.00)	0.4562
Female, n (%)	15 (60.00)	8 (44.44)	0.3246
Height (cm), median (range)	170.1 (164.4–176.5)	172.6 (167.1–180.8)	0.3883
Weight (kg), median (range)	72.40 (59.60–88.40)	78.30 (67.83–87.55)	0.2730
SCD type diagnosis			
SS/SC/SB0/SB + (n/n/n/n)	12/8/4/1	–	
Hematological indexes			
WBC (k/cumm), mean ± SD	9.23 ± 3.12	5.12 ± 1.55	< 0.0001****
RBC (million/cumm), mean ± SD	3.13 ± 0.78	4.67 ± 0.61	< 0.0001****
Hgb (GM/dL), mean ± SD	9.96 ± 1.94	13.44 ± 1.54	< 0.0001****
Hct (%), mean ± SD	28.88 ± 5.63	40.02 ± 4.30	< 0.0001****
Reticulocyte count (%), mean ± SD	5.76 ± 3.67	1.17 ± 0.43	< 0.0001****
Hemoglobin A %, mean ± SD	24.07 ± 13.02	94.79 ± 9.68	< 0.0001****
Hemoglobin S %, mean ± SD	64.71 ± 18.05	–	
Hemoglobin F %, mean ± SD	9.46 ± 7.89	–	
Disease-modifying therapy			
Chronic transfusion, n (%)	3 (12.00)	–	
Hydroxyurea, n (%)	15 (60.00)	–	
Patient-reported outcome measures			
BPI Pain Severity	3.854 ± 2.00	0.097 ± 0.4125	< 0.0001****
BPI Pain Interference	3.85 ± 2.12	–	
FPS Widespread Pain Index	5.28 ± 3.02	0.78 ± 1.59	< 0.0001****
HADS Depression Score	4.76 ± 3.09	1.94 ± 2.01	< 0.0021**
PROMIS-29 Physical Function	8.40 ± 3.82	4.50 ± 1.89	< 0.0001****
PedsQL Total Score	54.36 ± 11.61	–	

Table 1. Demographics.

SCD participants have lower median alpha frequencies in the resting state with eyes-closed

We first analyzed EEG data collected from 25 individuals with SCD and 18 HCs during an eyes-closed resting period. The average spectral power between the two groups showed that the alpha peak in SCD is shifted towards lower values (Fig. 2A). The shift in median alpha frequency occurred across the entire brain, and it was not localized to any specific regions. The SCD group exhibited a significantly lower ($p < 10^{-5}$) frequency of alpha waves (9.01 ± 0.09 Hz, Fig. 2B) compared to the control group (9.83 ± 0.13 Hz, Fig. 2B).

We calculated wPLI degree as the sum of weights attributed to the node, and there were no significant differences in the node-wise degree and mean degree of wPLI (Fig. 2C,D). However, in the pairwise wPLI, 3 pairs were significantly stronger, and 18 pairs were significantly weaker in SCD compared to HCs (Fig. 2C). To investigate if there is a difference in FDA between the two groups, we calculated the Spearman correlation ρ_f, and there were no significant differences between the SCD and control groups (Fig. 2E). Also, we could observe similar results under pain stimulation. The median alpha frequency significantly differed between HC and SCD groups ($p < 10^{-4}$) and SCD showed significantly lower wPLI for 14 pairs (Supplementary Fig. S3).

PROMs of SCD patients are associated with FDA during evoked pressure pain stimulation

The correlation between PROMs and FDA was examined for both resting and during cuff pain, using a partial correlation model that adjusted for age and sex. Partial correlations were made between frequency disassortativity and each PROMs: pain, depression, physical function, and pain-related quality of life. No significant correlations were found during resting state (all $p > 0.05$). In contrast significant correlations were observed during evoked cuff pain, where we found that ρ_f displayed a significant negative Spearman correlation with: BPI Pain Interference score ($\rho = -0.442$, $p = 0.039$), PROMIS29 Physical Function ($\rho = -0.664$, $p = 0.001$), and HADS Depression ($\rho = -0.493$, $p = 0.020$) in the SCD group (Table 2). The negative correlation between PROMs and ρ_f suggests that patients with greater pain, depression and poor physical function displayed greater ES features (Stronger FDA).

FDA during cuff pain is related to the occurrence of VOCs

We investigated the relationship between ES strength and VOCs by correlating the strength of FDA during cuff pain with the temporal proximity of VOCs. We classified the data into two groups based on time difference between the occurrence of crises and the EEG recording. If one or more crises occurred within 30 days before or after the EEG measurement date, that participant was assigned to the "close crisis" group, and if not, they were assigned to the "distant from crisis" group. We found that a statistically significant Spearman correlation coefficient between ρ_f and number of VOCs in the previous 12 months ($\rho = -0.5945$; $p = 0.0014$). Patients with a higher frequency of VOCs in the previous 12 months displayed stronger FDA (Fig. 3A). Importantly, the timing

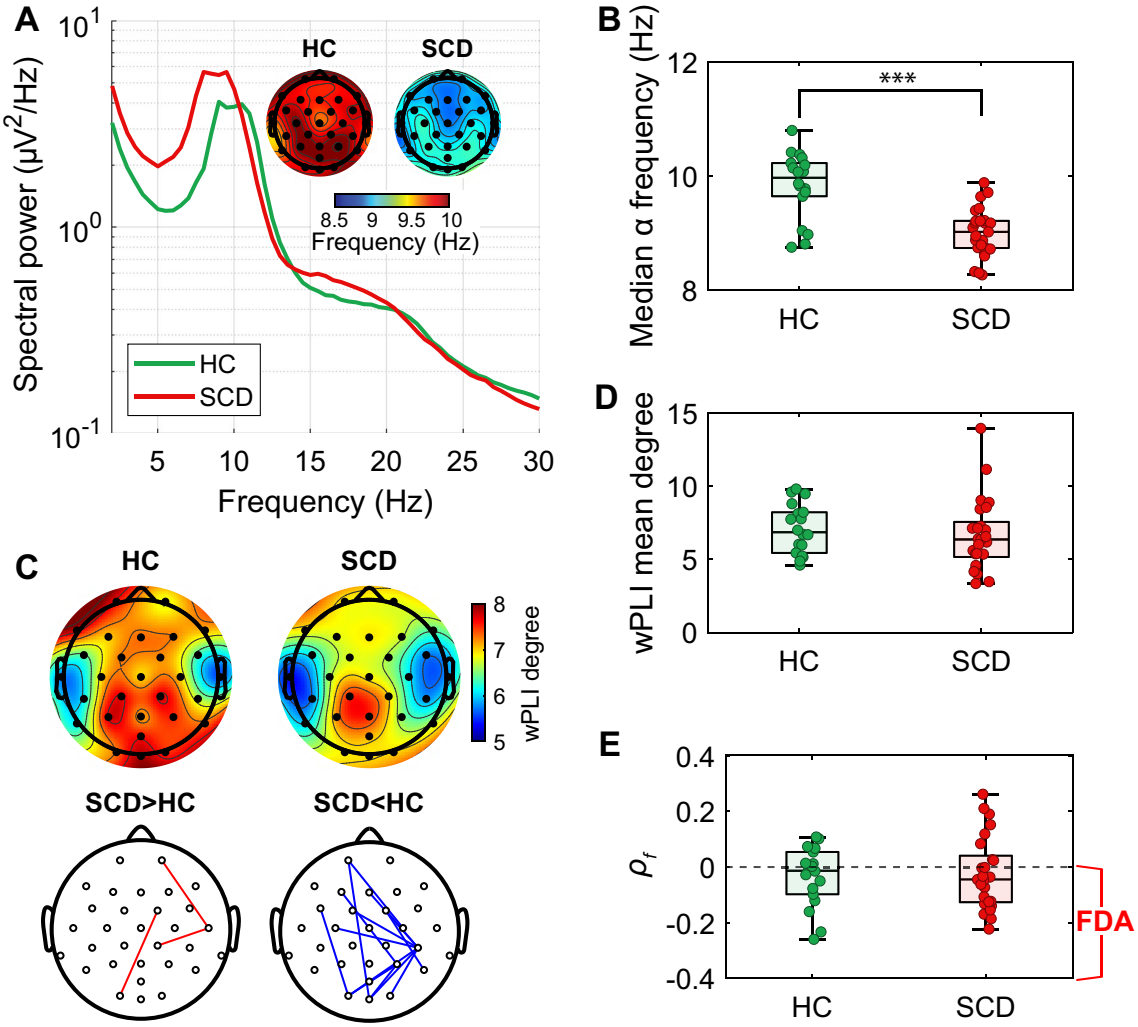

Figure 2. EEG characteristics in eye closed resting state. (**A**) EEG spectral power and topographic plots showing median alpha (7–13 Hz) frequency. (**B**) Topographic plot displaying wPLI degree and the significant difference of wPLI between HC and SCD. wPLI degree is calculated as the sum of weights attributed to the node. There was no significant difference in wPLI degree. Significantly stronger or weaker pairwise wPLI in SCD was indicated by red and blue lines, respectively. (**C**) Comparison of average median alpha frequencies between the HC and SCD groups. SCD group showed significantly lower median alpha frequency ($p < 10^{-5}$). (**D**) Mean values of node-wise wPLI degree was not significantly different. (**E**) FDA was not significantly different. ρ_f is Spearman correlation between median alpha frequencies and the average median alpha frequency of the connected nodes in the binarized wPLI network. The boxplots include horizontal lines indicating the 100%, 75%, 50%, 25%, and 0% percentiles. The statistics were derived from a two-sample t-test.

Patient reported outcomes	Spearman correlation (p-value)
BPI pain interference score	− 0.442 (0.039)*
BPI pain severity score	− 0.293 (0.186)
FPS widespread pain index	− 0.312 (0.157)
HADS depression score	− 0.493 (0.020)*
PROMIS-29 physical function score	− 0.664 (0.001)***
PedsQL total score	0.394 (0.069)

Table 2. Correlation between frequency disassortativity and patient reported clinical outcomes. Partial correlation model was constructed for frequency disassortativity and each of the patient-reported outcomes in pain, depression, physical function, and pain-related quality of life, with including age, sex and the use of hydroxyurea as covariables.

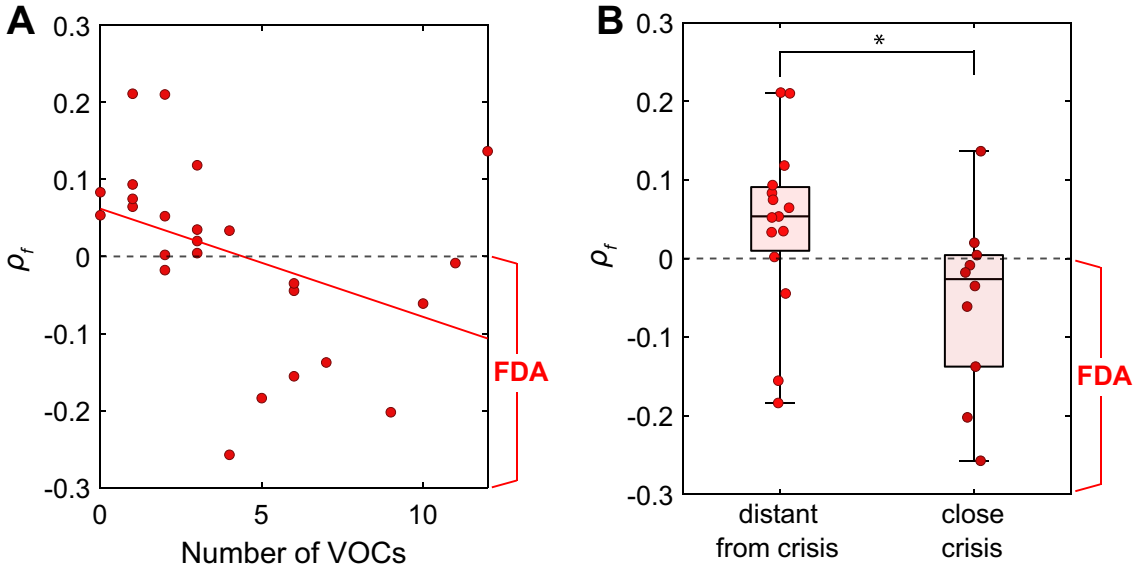

Figure 3. FDA predicts the occurrence of VOC. The relation between FDA calculated from EEG under stimulation and the occurrence of VOCs was analyzed. (**A**) The correlation between FDA and the number of VOCs in the previous 12 months was examined. A significant correlation was found between the number of VOCs and ρ_f. The red line indicates a linear regression. (**B**) The "close crisis" group showed significantly stronger FDA ($p = 0.04$) compared to the "distant from crisis" group. The boxplots include horizontal lines indicating the 100%, 75%, 50%, 25%, and 0% percentiles.

of VOC occurrence relative to EEG recordings was also significantly associated to the ES strength. The group of SCD patients that were in the "close crisis" group showed significantly stronger FDA compared to the "distant from crisis" group (Fig. 3B, Table 3). This implies that the closer the VOC occurrence is to the EEG recording, the stronger FDA.

Stronger ES strength leads to a more sensitive brain network and increased frequency of painful crises

To investigate the relationship between FDA and network sensitivity, we performed computational modeling on brain network dynamics. Using the DTI-based anatomical brain network consisting of Stuart-Landau oscillators, the responsivity and complexity under pulsatile stimulation were analyzed while varying FDA. Stronger model FDA was associated with higher responsivity and complexity of the model brain network after external perturbation (Fig. 4A,B), indicating that the model brain network exhibited increased sensitivity as it approached the strong ES.

To examine the relationship between the occurrence of VOCs and FDA, we simulated how brain networks with weak and strong ES strengths fluctuate in response to random perturbations on network coupling strength. Each model network received different perturbations at each 20-s step, and we observed changes in FDA amplitude over time (Fig. 4C). We observed that the frequencies of model "close crisis" states were higher when the initial FDA before perturbation was stronger (Fig. 4D), indicating that stronger FDA in the model was associated with a higher frequency of VOC occurrence.

Discussion

Overview of results

We analyzed EEG data from individuals with SCD with chronic pain and pain-free age- and gender-matched HCs at rest and during evoked experimental pressure pain. As seen in other chronic pain cohorts[21,40,41], the SCD group

Dependent variable	Predictor	Standard b	S.E. unstandardized	*P* value	R square full model
ρ_f	Close to OR distant from VOC	− 0.412	− 0.099	0.04	0.243
	Age	− 0.121	− 0.001	0.106	
	Sex	− 0.114	− 0.027	0.195	
	Hydroxyurea	− 0.218	− 0.052	0.213	

Table 3. FDA predicts the occurrence of VOC. Linear regression was constructed for frequency disassortativity with the time point that is relative to the occurrence of crisis ("close to or distant from VOC"), age, sex and the use of hydroxyurea as predictors.

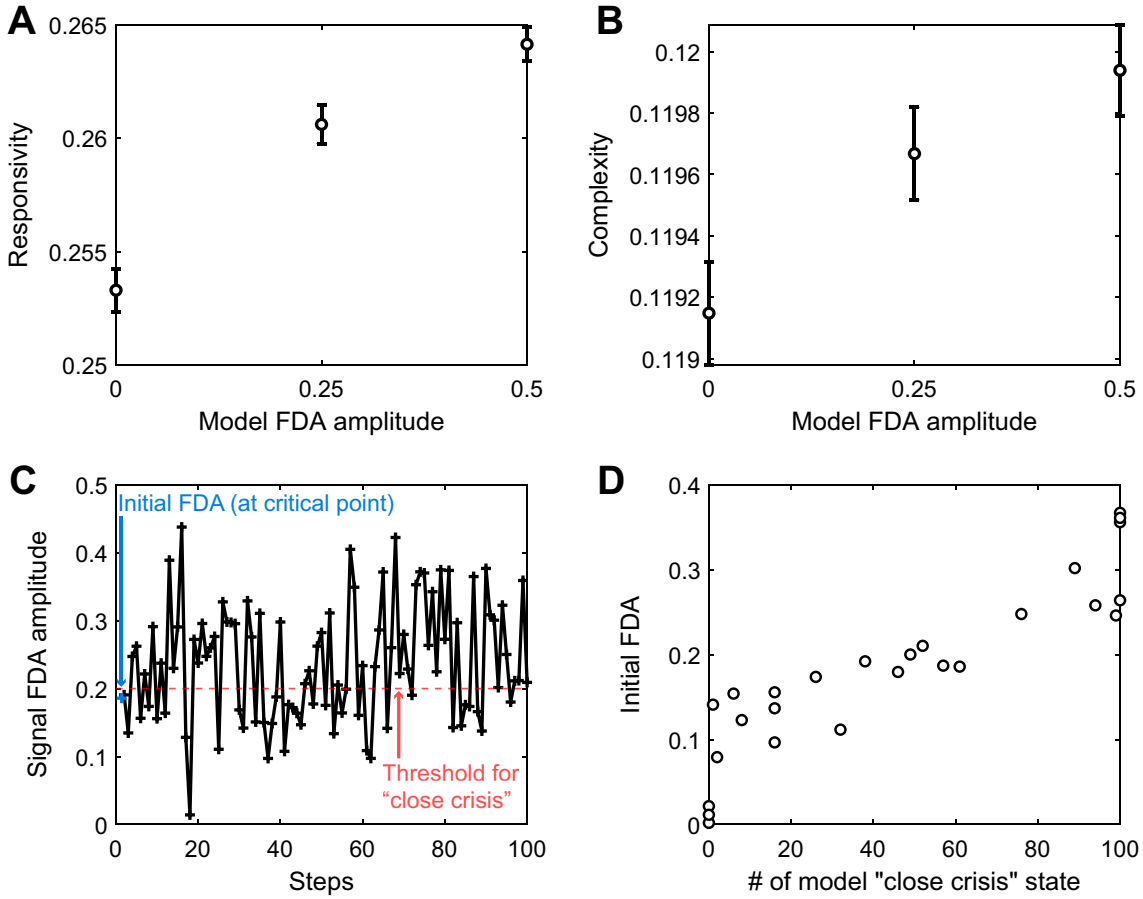

Figure 4. FDA explains sensitivity and frequency of "close crisis" states in the brain network model. A simulation was conducted to test the sensitivity of the model brain network. Global pulsatile stimulation was applied to the model brain network, and responsivity and complexity were measured from the perturbation response time series $PR_i(t)$. Another simulation was performed to investigate how random fluctuations in the coupling strength of the brain network can induce transitions to states of strong FDA. (**A**) The responsivity of the brain network to global pulsatile stimulation increases as FDA strengthened. (**B**) The Lempel–Ziv complexity of response time series after global pulsatile stimulation increases as FDA strengthened. (**C**) An example of stepwise simulation. Random perturbations are added to the coupling strength in the brain network for each step. (**D**) A higher initial FDA results in a more frequent incidence of model "close crisis" states. The Error bar represents the standard error of the mean.

exhibited a lower frequency of alpha waves compared to controls. No significant differences were found in the node-wise wPLI degree, but the pairwise wPLI exhibited lower values mainly in SCD. There were no significant differences in FDA between the groups during eyes-closed resting. However, during evoked pressure pain, the FDA of alpha waves in SCD was correlated with levels of pain interference, physical function, and depression. Patients with higher VOC frequency in the past 12 months also presented with stronger FDA, and closer occurrence of crises resulted in stronger frequency disassortativity in the SCD brain network.

We also sought to model the SCD brain network to examine FDA and its relationship to network instability. Computational modeling suggested that stronger FDA in our model was associated with higher responsivity and complexity, which indicated the increased sensitivity to the strong ES strength. We also investigated the occurrence frequency of VOCs by generating random fluctuations to the brain network. Interestingly, stronger initial FDA in the brain network led to higher VOC occurrence in our model, suggesting that the stronger frequency disassortativity may be associated with increased VOC occurrence in individuals with SCD.

Alpha EEG network and chronic pain in SCD

In this study, we focused on the alpha EEG band (7–13 Hz) for two key reasons. First, previous research in fibromyalgia, another chronic pain condition, demonstrated a significant correlation between the ES strength of the alpha EEG network and the pain scores[10]. We assumed that alpha waves might play a similar role in the SCD brain. Second, the typical large alpha power spectrum makes it easier to detect and define a representative frequency for each EEG channel, which is necessary for calculating frequency disassortativity. Recent studies have consistently reported on the relationship between pain intensity and alpha waves, primarily their power and frequency[21,42,43]. Theoretically, the alpha waves are thought to filter out irrelevant sensory inputs, enhance attentional focus, and enable efficient top-down control and the transfer of relevant information[44,45]. They may

also contribute to the coordination and synchronization of neural activities across different brain regions, facilitating effective information transfer and cognitive processing[46]. However, the mechanistic link of alpha waves to chronic pain is still elusive. Our EEG study suggests that the specific network configuration of globally interacting alpha waves, which is measured by frequency disassorativity, may create a heightened sensitivity to stimuli in the SCD brain. Furthermore, the mechanism of network sensitivity, ES, offers a mechanistic explanation for why SCD patients exhibit heightened pain responses compared to healthy individuals.

The mechanisms of VOC and chronic pain in SCD at a brain network level

The criticality hypothesis suggests that the brain in a conscious resting state resides near a critical state, which is a balanced state between order and disorder or between integration and segregation[32,35]. This means that the brain in a resting state is neither ordered (integrated) nor chaotic (segregated); therefore, it may be able to process information efficiently and effectively[34,47,48]. In thermodynamic systems, there are two types of phase transitions at critical points: the first-order phase transition (ES in a network) and the second-order phase transition (non-ES in a network). ES networks are characterized by higher sensitivity to stimuli and abrupt state transitions compared to lower sensitivity and gradual state transitions in non-ES networks[49]. In patients with SCD, we found that the degree of ES strength is positively correlated with self-reported pain measures and other related symptoms. We also found that as patients approach the onset of VOCs the degree of ES strength is also increased. Finally with computational modeling we demonstrated that the increased ES strength observed in SCD patients may enhance brain sensitivity as well as the frequency of crisis occurrence.

The accumulated effects of SCD within intervals between VOC occurrences may impact specific neural circuits and/or local brain regions altering the global brain network. Previous fMRI studies of SCD have consistently reported altered connectivity in the DMN, a primary hub structure in the global brain network[9,13,23]. Because the brain hub structure is a highly connected and centralized collection of nodes[22,40], we postulate that they are vulnerable to network attacks of accumulating neurobiological factors which may be operative in the SCD brain. Thus, an SCD patient in-between VOCs may accumulate neurobiological factors that promote ES properties mainly in hub structures (e.g., DMN), progressively developing an ES strength until the next VOC.

One possible explanation for the presence of strong ES in SCD patients could be due to weakened brain network efficiency. In line with our observation in this study, it is known that SCD patients display reduced efficiency and in their brain networks[50], which can lead to suppressed global synchronization and the potential emergence of strong ES within the network[49]. That is, weakened efficiency in brain connectivity may paradoxically contribute to the development of a hypersensitive network and excessive pain in SCD. In this study, we observed that the ES strength close in time to VOCs was stronger compared to a distant one. This may also suggest that as SCD patients approach VOC, the ES characteristics of their brain network become stronger. Also, our model demonstrates that strengthened frequency disassortativity enhances the sensitivity of the brain network, resulting in greater fluctuations in response to external perturbations. Consequently, this heightened sensitivity and increased fluctuations may raise the probability of encountering hazardous states like VOCs. Therefore, the larger variance in FDA within the SCD group and the frequent occurrence of crises among SCD patients can be attributed to the presence of a brain network that exhibits strong ES. The findings in this study provide support for our hypothesis that the increasing strength of ES in the SCD brain network is associated with the enlarging pain intensity observed during VOC progression (Fig. 5).

We found significant relationships only during the stimulation period, which could be attributed to variations in criticality. We assumed that the brain network in a conscious state resides at a critical point. However, recent empirical evidence suggests that the brain in a conscious resting state may not always stay at the exact critical point. Instead, it slightly deviates towards the sub-critical state (i.e., chaotic and segregated state)[51]. This prevents the brain from a sudden transition to a highly synchronized state (e.g., a seizure) by stochastic internal/external noises. Brain imaging studies have demonstrated that pain stimulation makes functional connectivity within parts of the brain stronger and integrative[52,53], and generally, increasing functional connectivity in a network can play a role in pushing a system in a sub-critical state (a segregated state) back closer to its critical point. Therefore, the pain stimulation may push the SCD brains closer to their critical points, making the difference between ES and non-ES more pronounced when they are near their critical points.

Explosive synchronization (ES) may be a novel marker of VOC onset and modulation

Over the last decade, many network configurations that can induce ES have been discovered, including: (1) positive correlation between node degrees and node frequencies, (2) negative frequency assortativity (a tendency of high-frequency nodes to be linked with low-frequency nodes), (3) large frequency difference, (4) random connectivity, and (5) negative feedback process among nodes[49,54,55]. Our findings indicate the potential of FDA as a predictor for VOCs in SCD. FDA was first shown to have a correlation with pain in fibromyalgia[10]. Here, we observe positive correlations between the strength of ES and symptoms of pain and depression in SCD patients, while no significant correlations were found for other ES conditions. The consistency of FDA across diverse pain conditions, including fibromyalgia and SCD, implies its potential as a predictive measure for pain, irrespective of underlying mechanisms of pain. This may allow the finding of better ES conditions that can reflect the pain scores and predict the upcoming pain crisis. This needs further study to develop the network principle-based prediction system of pain crises.

ES can provide a theoretical framework for the treatment of SCD pain through network modulation

Discovering correlations between ES strength in the SCD brain, pain intensity, and frequency of VOCs could help us develop a novel treatment method to reduce pain intensity and frequency of pain crises. In a recent

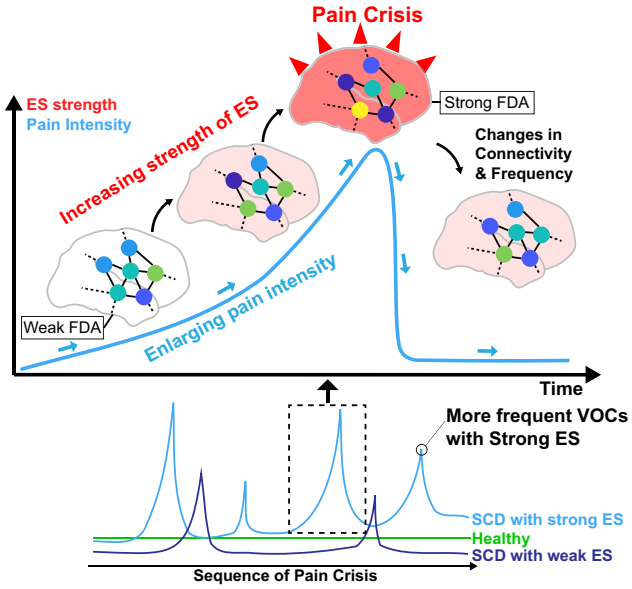

Figure 5. Hypothesis on the network mechanism of pain and VOCs in SCD. The effect of SCD may gradually accumulate within the brain network, strengthening FDA, an ES condition. The cumulative effect on ES can enhance the sensitivity of brain network and upon reaching a critical threshold, potentially triggering a crisis upon reaching a critical threshold. The difference in node colors in the brain network indicates the difference in node frequencies.

computational model, we showed that increasing connectivity in hub regions (e.g., insula, isthmus cingulate cortex, and precuneus) in an ES brain network can convert it into a non-ES brain network[11], which significantly reduces the brain's sensitivity to external stimuli. Our next step is to apply a stimulation method (e.g., acupuncture or transcranial direct current stimulation) that is known to alter brain connectivity[56,57] to our modeling approach. Based on the computational study and our empirical findings in SCD, we could develop a novel theoretical basis for systematically predicting and modulating pain intensity as well as the frequency of VOCs by converting the type of phase transition in individual SCD patients' brains.

Limitations

Our study offers valuable insights into brain network mechanisms of VOCs in SCD; however, it also has certain limitations. In analytic and modeling studies, frequency disassortativity in a network is defined by the initial arrangement of frequencies (called natural frequencies) to the nodes. However, we cannot directly measure natural frequencies in brain regions using EEG data. Furthermore, we determined the median frequency from the band EEG, ignoring the spectral distribution. This simplification in sensor signals may not accurately reflect the real-brain network dynamics in source signals. Simultaneous recordings of fMRI and EEG may enable us to estimate the strength of ES more precisely. Finally, the amount of data recorded near the onset of VOCs was also largely restricted by the number of VOCs naturally occurring that were adjacent to the recording time. Due to this limitation of not knowing precisely when a VOC is going to occur prospectively, there is a significant challenge in using EEG to study or clinically manage VOCs.

Conclusion

The present study establishes a significant link between pain in SCD and a universal network mechanism, ES. It offers a robust theoretical foundation for comprehending pain in SCD through the brain network mechanism. This enhanced understanding will facilitate future investigations on predicting pain crises and refining pain management strategies for SCD patients.

Data availability

The data that support the findings of this study are available on request from the corresponding author upon reasonable request. The data are not publicly available due to privacy or ethical considerations.

Received: 28 November 2023; Accepted: 18 March 2024
Published online: 27 March 2024

References

1. Karafin, M. S. *et al.* Predictive factors of daily opioid use and quality of life in adults with sickle cell disease. *Hematology* **23**, 856–863 (2018).

2. Zaidi, A. U. *et al.* A systematic literature review of frequency of vaso-occlusive crises in sickle cell disease. *Orphanet. J. Rare Dis.* **16**, 460 (2021).
3. Chalacheva, P. *et al.* Biophysical markers of the peripheral vasoconstriction response to pain in sickle cell disease. *PLoS One* **12**, e0178353 (2017).
4. Shah, P. *et al.* Mental stress causes vasoconstriction in subjects with sickle cell disease and in normal controls. *Haematologica* **105**, 83–90 (2020).
5. Thuptimdang, W. *et al.* Vasoconstriction response to mental stress in sickle cell disease: The role of the cardiac and vascular baroreflexes. *Front. Physiol.* **12**, 698209 (2021).
6. Wang, Y. *et al.* Alteration of grey matter volume is associated with pain and quality of life in children with sickle cell disease. *Transl. Res.* **240**, 17–25 (2022).
7. Harris, R. E. *et al.* Pregabalin rectifies aberrant brain chemistry, connectivity, and functional response in chronic pain patients. *Anesthesiology* **119**, 1453–1464 (2013).
8. Harte, S. E., Harris, R. E. & Clauw, D. J. The neurobiology of central sensitization. *J. Appl. Biobehav. Res.* **23**, e12137 (2018).
9. Gómez-Gardeñes, J., Gómez, S., Arenas, A. & Moreno, Y. Explosive synchronization transitions in scale-free networks. *Phys. Rev. Lett.* **106**, 128701 (2011).
10. Lee, U. *et al.* Functional brain network mechanism of hypersensitivity in chronic pain. *Sci. Rep.* **8**, 243 (2018).
11. Kim, M., Harris, R. E., DaSilva, A. F. & Lee, U. Explosive synchronization-based brain modulation reduces hypersensitivity in the brain network: A computational model study. *Front. Comput. Neurosci.* **16**, 815099 (2022).
12. Kim, J. *et al.* The somatosensory link in fibromyalgia: functional connectivity of the primary somatosensory cortex is altered by sustained pain and is associated with clinical/autonomic dysfunction. *Arthritis Rheumatol.* **67**, 1395–1405 (2015).
13. Campbell, C. M. *et al.* An evaluation of central sensitization in patients with sickle cell disease. *J. Pain* **17**, 617–627 (2016).
14. Curtis, S. & Brandow, A. M. Responsiveness of Patient-Reported Outcome Measurement Information System (PROMIS) pain domains and disease-specific patient-reported outcome measures in children and adults with sickle cell disease. *Hematology* **2017**, 542–545 (2017).
15. Clauw, D. Fibromyalgia: A clinical review. *JAMA* **311**, 1547–1555 (2014).
16. Dudeney, J., Law, E. F., Meyyappan, A., Palermo, T. M. & Rabbitts, J. A. Evaluating the psychometric properties of the widespread pain index and the symptom severity scale in youth with painful conditions. *Can. J. Pain* **3**, 137–147 (2019).
17. Darbari, D. S. *et al.* Frequency of hospitalizations for pain and association with altered brain network connectivity in sickle cell disease. *J. Pain* **16**, 1077–1086 (2015).
18. Panepinto, J. A. *et al.* PedsQL™ sickle cell disease module: Feasibility, reliability, and validity. *Pediatr. Blood Cancer* **60**, 1338–1344 (2013).
19. Delorme, A. & Makeig, S. EEGLAB: an open source toolbox for analysis of single-trial EEG dynamics including independent component analysis. *J. Neurosci. Methods* **134**, 9–21 (2004).
20. Pion-Tonachini, L., Kreutz-Delgado, K. & Makeig, S. ICLabel: An automated electroencephalographic independent component classifier, dataset, and website. *NeuroImage* **198**, 181–197 (2019).
21. Furman, A. J. *et al.* Sensorimotor peak alpha frequency is a reliable biomarker of prolonged pain sensitivity. *Cereb. Cortex* **30**, 6069–6082 (2020).
22. Klimesch, W. EEG alpha and theta oscillations reflect cognitive and memory performance: A review and analysis. *Brain Res. Rev.* **29**, 169–195 (1999).
23. Peng, W., Babiloni, C., Mao, Y. & Hu, Y. Subjective pain perception mediated by alpha rhythms. *Biol. Psychol.* **109**, 141–150 (2015).
24. Ploner, M., Sorg, C. & Gross, J. Brain rhythms of pain. *Trends Cogn. Sci.* **21**, 100–110 (2017).
25. Vinck, M., Oostenveld, R., van Wingerden, M., Battaglia, F. & Pennartz, C. M. A. An improved index of phase-synchronization for electrophysiological data in the presence of volume-conduction, noise and sample-size bias. *Neuroimage* **55**, 1548–1565 (2011).
26. Leyva, I. *et al.* Explosive synchronization in weighted complex networks. *Phys. Rev. E* **88**, 042808 (2013).
27. Zhu, L., Tian, L. & Shi, D. Criterion for the emergence of explosive synchronization transitions in networks of phase oscillators. *Phys. Rev. E* **88**, 042921 (2013).
28. Cabral, J., Fernandes, F. F. & Shemesh, N. Intrinsic macroscale oscillatory modes driving long range functional connectivity in female rat brains detected by ultrafast fMRI. *Nat. Commun.* **14**, 375 (2023).
29. Deco, G., Liebana Garcia, S., Sanz Perl, Y., Sporns, O. & Kringelbach, M. L. The effect of turbulence in brain dynamics information transfer measured with magnetoencephalography. *Commun. Phys.* **6**, 1–8 (2023).
30. van den Heuvel, M. P. & Sporns, O. Rich-club organization of the human connectome. *J. Neurosci.* **31**, 15775–15786 (2011).
31. Caminiti, R. *et al.* Diameter, length, speed, and conduction delay of callosal axons in macaque monkeys and humans: Comparing data from histology and magnetic resonance imaging diffusion tractography. *J. Neurosci.* **33**, 14501–14511 (2013).
32. Beggs, J. M. The criticality hypothesis: How local cortical networks might optimize information processing. *Philos. Trans. R. Soc. A Math. Phys. Eng. Sci.* **366**, 329–343 (2007).
33. Kim, H. & Lee, U. Criticality as a determinant of integrated information Φ in human brain networks. *Entropy* **21**, 981 (2019).
34. Kim, M. *et al.* Criticality creates a functional platform for network transitions between internal and external processing modes in the human brain. *Front. Syst. Neurosci.* **15**, (2021).
35. Tian, Y. *et al.* Theoretical foundations of studying criticality in the brain. *Netw. Neurosci.* **6**, 1148–1185 (2022).
36. Yoon, S., Sorbaro Sindaci, M., Goltsev, A. V. & Mendes, J. F. F. Critical behavior of the relaxation rate, the susceptibility, and a pair correlation function in the Kuramoto model on scale-free networks. *Phys. Rev. E* **91**, 032814 (2015).
37. Skardal, P. S., Restrepo, J. G. & Ott, E. Frequency assortativity can induce chaos in oscillator networks. *Phys. Rev. E* **91**, 060902 (2015).
38. Kim, M. & Lee, U. Alpha oscillation, criticality, and responsiveness in complex brain networks. *Netw. Neurosci.* **4**, 155–173 (2020).
39. Lempel, A. & Ziv, J. On the complexity of finite sequences. *IEEE Trans. Inf. Theory* **22**, 75–81 (1976).
40. Furman, A. J. *et al.* Cerebral peak alpha frequency predicts individual differences in pain sensitivity. *NeuroImage* **167**, 203–210 (2018).
41. de Vries, M. *et al.* Altered resting state EEG in chronic pancreatitis patients: Toward a marker for chronic pain. *JPR* **6**, 815–824 (2013).
42. Zebhauser, P. T., Hohn, V. D. & Ploner, M. Resting-state electroencephalography and magnetoencephalography as biomarkers of chronic pain: A systematic review. *PAIN* **164**, 1200 (2023).
43. Sarnthein, J., Stern, J., Aufenberg, C., Rousson, V. & Jeanmonod, D. Increased EEG power and slowed dominant frequency in patients with neurogenic pain. *Brain* **129**, 55–64 (2006).
44. Klimesch, W. α-band oscillations, attention, and controlled access to stored information. *Trends Cogn. Sci.* **16**, 606–617 (2012).
45. Halgren, M. *et al.* The generation and propagation of the human alpha rhythm. *Proc. Natl. Acad. Sci.* **116**, 23772–23782 (2019).
46. Alamia, A. & VanRullen, R. Alpha oscillations and traveling waves: Signatures of predictive coding?. *PLOS Biol.* **17**, e3000487 (2019).
47. Popiel, N. J. M. *et al.* The emergence of integrated information, complexity, and 'consciousness' at criticality. *Entropy* **22**, 339 (2020).
48. Shine, J. M., Aburn, M. J., Breakspear, M. & Poldrack, R. A. The modulation of neural gain facilitates a transition between functional segregation and integration in the brain. *eLife* **7**, e31130 (2018).

49. Boccaletti, S. *et al.* Explosive transitions in complex networks' structure and dynamics: Percolation and synchronization. *Phys. Rep.* **660**, 1–94 (2016).
50. Case, M. *et al.* Graph theory analysis reveals how sickle cell disease impacts neural networks of patients with more severe disease. *NeuroImage: Clin.* **21**, 101599 (2019).
51. Priesemann, V. *et al.* Spike avalanches in vivo suggest a driven, slightly subcritical brain state. *Front. Syst. Neurosci.* **8** (2014).
52. Kastrati, G., Thompson, W. H., Schiffler, B., Fransson, P. & Jensen, K. B. Brain network segregation and integration during painful thermal stimulation. *Cereb. Cortex* **32**, 4039–4049 (2022).
53. Seminowicz, D. A. & Davis, K. D. Pain enhances functional connectivity of a brain network evoked by performance of a cognitive task. *J. Neurophysiol.* **97**, 3651–3659 (2007).
54. Filatrella, G., Pedersen, N. F. & Wiesenfeld, K. Generalized coupling in the Kuramoto model. *Phys. Rev. E* **75**, 017201 (2007).
55. Kim, H., Moon, J.-Y., Mashour, G. A. & Lee, U. Mechanisms of hysteresis in human brain networks during transitions of consciousness and unconsciousness: Theoretical principles and empirical evidence. *PLOS Comput. Biol.* **14**, e1006424 (2018).
56. Cai, R., Shen, G., Wang, H. & Guan, Y. Brain functional connectivity network studies of acupuncture: A systematic review on resting-state fMRI. *J. Integr. Med.* **16**, 26–33 (2018).
57. Kunze, T., Hunold, A., Haueisen, J., Jirsa, V. & Spiegler, A. Transcranial direct current stimulation changes resting state functional connectivity: A large-scale brain network modeling study. *NeuroImage* **140**, 174–187 (2016).

Acknowledgements

The authors would like to thank Brandon Alec Reyes, Tyler James Barret, Nayana Dutt, Payton Mittman, Bea Paras and Amy Gao for assisting with experimental performance; Siddhi Gandhi, Charanjit Kaur, and Veena Vijayan for data management and validation, as well as all the providers affiliated with Indiana University Health and Indiana Hemophilia & Thrombosis Center for patient referral to this study. The authors also thank Indiana University Clinical Research Center for resource support. This work was supported by NIH K99/R00 award (Grant # 4R00AT010012) and Indiana University Health—Indiana University School of Medicine Strategic Research Initiative funding to YW. UL was supported by NIGMS (R21GM143521).

Author contributions

PJ, REH, UL and YW analyzed and interpreted the data and drafted the manuscript; MK assisted with data analyses and interpretation; PJ and UL conducted computational modeling; BK, VV and YT assisted with data collection; ZYL provided statistical assistance; SEH, REH, UL, and YW edited the manuscript; ARW and YW directed patient recruitment; YW directed the experimental performance, data collection and quality of the clinical investigation.

Competing interests

SEH has consulted for Aptinyx, Memorial Sloan Kettering Cancer Institute, University of North Carolina-Chapel Hill, Indiana University, and University of Glasgow, and has received research funding from NIH, Arbor Medical Innovations, and Aptinyx. REH has received grant funding from Pfizer, Aptinyx, and Cerephex and National Institutes of Health (NIH). The remaining authors declare no competing interests.

Additional information

Supplementary Information The online version contains supplementary material available at https://doi.org/10.1038/s41598-024-57473-5.

Correspondence and requests for materials should be addressed to U.L. or Y.W.

Reprints and permissions information is available at www.nature.com/reprints.

Publisher's note Springer Nature remains neutral with regard to jurisdictional claims in published maps and institutional affiliations.